SCALING OF POST-CONTRACTILE PHOSPHOCREATINE RECOVERY IN WHITE MUSCLE OF BLACK SEA BASS, *CENTROPRISTIS STRIATA*

Albert C. Nyack

A Thesis Submitted to the
University of North Carolina Wilmington in Partial Fulfillment
Of the Requirements for the Degree of
Masters of Science

Department of Biology and Marine Biology

University of North Carolina Wilmington

2006

Approved by

Advisory Committee

_____ _____

_____
Chair

Accepted by

_____
Dean, Graduate School

This thesis has been prepared in the style and format

consistent with the journal

Journal of Experimental Biology

TABLE OF CONTENTS

ABSTRACT

During somatic growth, increases in fish muscle mass occur both by hyperplasia and hypertrophy, and in some species the hypertrophic phase of growth leads to very large fiber diameters. Large fiber size leads is associated with low fiber surface area to volume (SA:V), which may (1) limit O_2 flux across the sarcolemmal, (2) create potentially large intracellular diffusion distances between mitochondria, and (3) lead to diffusive constraints on aerobic metabolism. This study examined the effects of intracellular metabolite diffusion by investigating how the rate of post-contractile phosphocreatine (PCr) recovery in isolated epaxial white muscle from black sea bass (*Centropristis striata*) scales with body mass (and fiber size). Isolated muscle fibers from different sized fish (5.7 to 4159.4 g) were stimulated until PCr was depleted. The use of isolated fiber bundles in a high PO_2 superfusion medium eliminated the confounding effects of fiber SA:V on oxygen flux across the membranes. Light microscopy and transmission electron microscopy techniques were employed to characterize fiber size and intracellular structure. White muscle fiber diameters increased significantly during growth, and became very large in adult fish (>250 μm). Mitochondrial density and cytochrome-*c* oxidase (COX) activity scaled negatively with increasing body mass, and had similar scaling exponents to each other. Sub-sarcolemmal mitochondrial volume per sarcolemmal membrane area significantly increased during fiber growth, indicating a shift in mitochondria towards areas of higher PO_2 at the periphery of the fiber. Despite differences in fiber size, aerobic capacity, and intracellular diffusion distances between size classes, the post-contractile recovery rate of PCr was size independent. Further, a mathematical reaction-diffusion analysis indicated that the rate of PCr resynthesis was too slow to be limited by intracellular metabolite diffusion. These results suggest that in these white fibers, the rate of PCr recovery is limited by the low mitochondrial

density. Additionally, the change in mitochondrial distribution with increasing fiber size suggests that low SA:V and limited O_2 flux is a more important design constraint in large fibers of fish white muscle than is intracellular metabolite flux.

ACKNOWLEDGEMENTS

I sincerely thank my advisor, Dr. Stephen Kinsey, for his guidance, support, tolerance, and humor during my graduate career. His scientific (and life) insights and dedication to helping me succeed will always be deeply appreciated. I also thank Dr. D. Ann Pabst whose efforts and encouragements, both as my committee member and graduate coordinator, have made the graduate experience invaluable. The enthusiasm and thoughtfulness from Dr. Thomas Lankford prior to beginning graduate school, and as a committee member, never ceased to amaze me. Thank you T. I would also like to extend my sincerest gratitude to Mark Gay and Dr. Dillaman for the crash course in microscopy techniques and for providing a surrogate lab for a summer. Finally, this work would not have been possible without the aid of Dr. Watanabe and the gentlemen at the aquaculture facility: Pat Carroll, Troy Rezek, and Chris Bentley. Thank you for your cooperation and patience.

I would also like to thank previous members of our lab, Lisa Johnson and Soma Sarkar. Their combination of hard work and camaraderie was unique and inspiring, and they are truly missed. My current lab-mates, Kristin Hardy, Jennifer Berting, Jeff Overton, and Ana Jimenez have made life more than interesting and I value the experiences we shared, especially playing in the sand.

I would also like to thank my family, who has been there to support and congratulate me through it all. My deepest thanks go to my wife, Kristen Andrews; I don't know where I would be without her.

Finally, I would like to acknowledge the National Science Foundation for supporting this research and my experience as a GK-12 Fellow.

LIST OF TABLES

LIST OF FIGURES

INTRODUCTION

Studies of the scaling of metabolism with increasing body mass historically have focused on rates of whole animal O_2 consumption (reviewed in Schmidt-Nielsen, 1984). More recently, a mechanistic basis for scaling of metabolic rate has been proposed that is rooted in the fractal branching pattern of energy distribution networks in organisms (West *et al.* 1999). At the tissue level, the scaling of the activity of aerobic and anaerobic enzymes, such as cytochrome-*c* oxidase (COX) and lactate dehydrogenase (LDH), respectively, has been well studied in fish muscle (Somero and Childress, 1980; Somero and Childress, 1990; Childress and Somero, 1990; Goolish, 1991; Norton *et al.* 2000). While these studies yield indices of tissue metabolic capacity, the processes that are powered by aerobic energy metabolism have been largely neglected. It has been assumed that aerobic capacity and aerobic processes scale in parallel, but changes in cellular dimensions and metabolic organization with increasing body mass may cause these metabolic rate indicators to scale independently.

Divergence in the scaling of rates of energy metabolism and the processes it supports might be particularly prevalent in fish white muscle fibers, which can greatly exceed the 10 to 100 μm diameter size range adhered to by most vertebrate muscle fibers (Russell *et al.* 2000). For the majority of fish species, axial white muscle comprises most of the body mass (Valente *et al.* 1999; Mommsen, 2001) and increases in fish muscle mass occur by both hyperplasia and hypertrophy (Weatherly and Gill, 1985; Koumans and Akster, 1995; Onali *et al.* 1996; Valente *et al.* 1999). Although there is some controversy about the relative contribution of hyperplasia and hypertrophy to fish muscle growth, Veggetti *et al.* (1990) suggested that in adult sea bass (*Dicentrarchus labrax*) hypertrophy is the predominant form of increasing muscle mass. In some species of fish, notably in Notothenioids, axial white muscle hypertrophy can proceed until fibers

diameters greatly exceed 100 μm (Battram and Johnston, 1991; Fernandez, 2000; Johnston *et al.* 2003). However, the impacts of developing large muscle fibers on metabolism are still not well understood (Johnston *et al.* 2004; Kinsey *et al.* 2005).

Prolonged periods of hypertrophy during development are not uncommon, and have also been observed during growth of anaerobic muscle fibers from crustaceans (Tse *et al.* 1983; Boyle *et al.* 2003; Johnson *et al.* 2004). For instance, during the development of the blue crab, *Callinectes sapidus*, the anaerobic muscle fibers in the swimming leg increase from < 100 μm in small crabs to > 500 μm in adults, and mitochondrial distribution shifts from a uniform intracellular distribution to one that is predominantly sub-sarcolemmal (Boyle *et al.* 2003). This mitochondrial shift appears to be in response to limited O_2 flux due to a low fiber SA:V, but occurs at the expense of increased intracellular diffusion distances between mitochondrial clusters and sarcoplasmic ATPases, which may limit aerobic processes (Boyle *et al.* 2003; Johnson *et al.* 2004).

The burst contractile function of muscle is an anaerobic process and therefore is not dependent on oxygen flux across the cell membrane or intracellular metabolite diffusive flux to meet ATP demand (Dobson and Hochachka, 1987; reviewed in McMahon and Jenkins, 2002; reviewed in Suarez, 2003). In fish white muscle, intracellular stores of phosphocreatine (PCr) exceed those of ATP and are the initial source of high-energy phosphates during burst contraction (Dobson and Hochachka, 1987; Schulte *et al.* 1992; Hochachka and Mossey, 1998; Richards *et al.* 2003). The creatine kinase (CK) reaction catalyses the reversible transfer of a phosphoryl group from PCr to ADP forming ATP:

$$PCr + ADP + \alpha H^+ \overset{CK}{\longleftrightarrow} Cr + ATP$$

where α represents a partial proton and Cr is creatine (e.g. Hochachka and Mossey, 1998). The high activity of this reaction in burst muscle and the several fold greater intracellular [PCr] than [ATP] indicates that PCr acts to buffer [ATP] during muscle contractions (Moon *et al.* 1991; Hochachka and Mossey, 1998; reviewed in Kushmerick, 1998; McMahon and Jenkins, 2002). During recovery from contraction, however, ATP and PCr resynthesis occurs aerobically in fish muscle (Curtin *et al.* 1997), and the majority of high-energy phosphate flux from the mitochondria to the rest of the cell is again mediated by the CK reaction, with PCr as the dominant diffusing species (Fig. 1; Mainwood and Rakusan, 1982; Meyer *et al.* 1984; Ellington and Kinsey, 1998). Thus, the recovery rate of PCr is tightly coupled to both the aerobic production of ATP at the mitochondria and the diffusive flux of Cr/PCr.

The intracellular domain within muscle fibers is crowded with both soluble proteins and fixed structures such as mitochondria, sarcoplasmic reticulum (SR), and myofilaments (Kay *et al.* 1997; reviewed in Lindstedt *et al*. 1998; Kinsey and Moerland, 2002; reviewed in Suarez, 2003) and these obstacles reduce the diffusive flux of small metabolites, such as PCr and ATP (Jacobson and Wojcieszyn, 1984; Meyer, 1988; Meyer, 1989; Hubley *et al.* 1997; Kinsey *et al.* 1999; Kinsey and Moerland, 2002; Kinsey *et al.* 2005). Further, Kinsey *et al.* (1999) and Kinsey and Moerland (2002) found that the radial diffusion coefficient, *D*, which is the direction of diffusive flux relevant to energy metabolism, is time-dependent, and they inferred from mathematical modeling that the impedance at greater diffusion times is principally caused by the sarcoplasmic reticulum (SR). Thus, at the short intracellular diffusion distances characteristic of small cells, the radial diffusion coefficient is greater than that of the large diffusion distances that may be prevalent in large cells. The reduced rate of radial diffusive flux, coupled with potentially

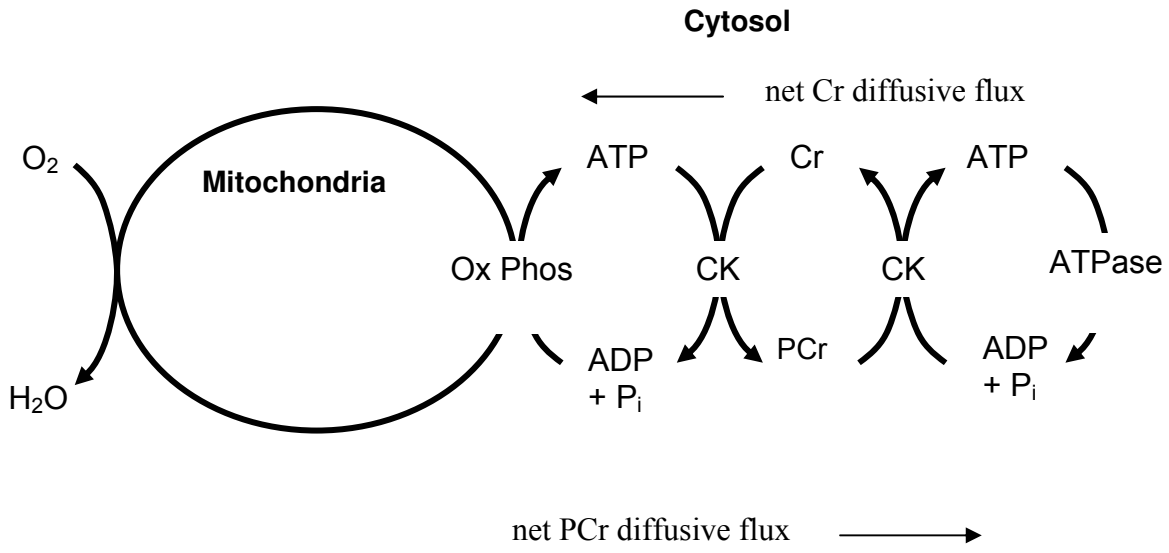

Figure 1. A representation of diffusive flux facilitated by creatine kinase. Increased diffusion distances in large fish may lead to diffusion limitations on PCr/Cr flux.

extreme diffusion distances in large fibers of fish white muscle, may impact how the rate of post-contractile PCr recovery scales with body mass.

Several studies have previously hypothesized that diffusion constraints are the cause underlying the recruitment of anaerobic metabolism following burst contractions in the very large muscle fibers of adult crustaceans (Kinsey and Moerland, 2002; Boyle *et al.* 2003; Johnson *et al.* 2004). Kinsey *et al.* (2005) tested this hypothesis by comparing the scaling with body mass of post-contractile recovery rates of arginine phosphate (AP) in the anaerobic swimming muscle of *C. sapidus* to a mathematical reaction-diffusion model of aerobic metabolism in crab fibers. They concluded that intracellular metabolite diffusion did not limit the rate of AP recovery in large fibers, and suggested that SA:V and the associated constraints on O_2 flux exerted more influence over intracellular metabolic fluxes and metabolic design. However, their study was conducted using an *in vivo* exercise protocol, where the effects of fiber size could lead to limited metabolic flux due to (1) large intracellular diffusion distances, (2) low SA:V, or (3) a combination of both factors.

The present study was designed to test the conclusions drawn by Kinsey *et al.* (2005) by assessing only the effects of intracellular metabolite diffusion on aerobic metabolism. I examined how the post-contractile PCr recovery rate (a *product* of aerobic respiration) in isolated white muscle preparations from black sea bass, *Centropristis striata* scaled with body mass. The use of isolated muscle fiber bundles superfused in a high PO_2 environment removed the potential effects of low fiber SA:V on limitations to O_2 flux. This method allowed examination of only the effects of intracellular diffusion on metabolite recovery. Muscle fiber growth was characterized by measuring fiber diameter over a large range of body mass, which has not been previously done in *C. striata*. Aerobic capacity was analyzed by measuring mitochondrial volume density

and COX activity, and changes in mitochondrial distribution were examined during hypertrophic muscle growth. I hypothesized that there would be an increase in the sub-sarcolemmal mitochondrial clustering during hypertrophic growth, resulting in increased radial diffusion distances between mitochondrial clusters. Further, the rate of post-contractile PCr resynthesis was expected to be lowest in muscle from the largest animals as a consequence of increased diffusion distances associated with hypertrophic fiber growth. Despite finding a large increase in fiber size during development, and an increase in sub-sarcolemmal mitochondrial volume per membrane area, there were no differences in the rate of PCr recovery among size classes. Further, the rate of post-contractile PCr recovery was too slow to be limited by intracellular metabolite diffusion. These results suggest that (1) PCr recovery is largely limited by the low mitochondrial density and (2) fiber SA:V is a more important mediator of aerobic flux and metabolic design than intracellular metabolite diffusion in large white fibers from fish.

MATERIALS AND METHODS

Animal Maintenance

Centropristis striata from three size classes, designated as small (<25 g), medium (50 to 750 g), and large (> 1000 g) based on body mass, were obtained from the UNCW Aquaculture Facility at Wrightsville Beach, NC. While at the aquaculture facility, fish were reared in controlled environments (22-25 °C, pH 7.8-8.3, salinity >30 ppt), maintained on a 14:10 h light-dark cycle, and fed a diet of pellets containing 45% protein 6% fat. At least 24 h before experiments, fish were transported in large coolers to tanks at UNCW's main campus and maintained under the same conditions until use.

Muscle Preparation

The following general protocol was used to prepare excised anterior dorsolateral, epaxial

white muscle tissue for the fiber size, mitochondrial distribution, and phosphocreatine recovery (PCr) experiments, with specific alterations described in each section. To avoid muscle PCr depletion due to handling stress, animals were individually sequestered for at least 1 h prior to sacrifice in covered and aerated opaque containers with minimal water volume to limit movement. Animals were tranquilized with concentrated MS-222 (tricaine methanesulfonate; Argent Laboratories, Redmond, WA) that was gently diluted to 500 $mg \cdot L^{-1}$ (final volume) in the container's seawater via a small hole in the container cover to minimize disturbance of the fish. Fish remained in the container until they were non-responsive to gentle prodding and/or they lost equilibrium control. Sedating fish with MS-222 prior to NMR experiments is a common technique that has been shown not to interfere with high-energy phosphate concentration in living tissue (Moerland and Egginton, 1998), and rapidly flushes out of an organism's muscle tissue upon soaking in untreated water (manufacturer's technical specification).

Fish body mass and total length (TL) was recorded, and anesthetized animals were sacrificed via cervical dislocation to minimize neural-muscular contractions during dissection. The anterior dorsolateral body surface, dorsal to the operculum and just below and anterior to the dorsal fin, on both sides of the animal was scaled. Two rectangular section of skin in the scaled region, one on each side of the dorsal median, were quickly cut and reflected posteriorly. Strips of epaxial white muscle, undamaged by dermal reflection, were excised parallel to the fiber's long axis orientation, and maintained *ex vivo* in saline solution (composition in $mM \cdot L^{-1}$: 133.5 NaCl, 2.4 KCl, 11.3 $MgCl_2$, .47 $CaCl_2$, 18.5 $NaHCO_3$, 3.2 NaH_2PO_4, pH 7.4) aerated with a mixture of 99.5% O_2 and 0.5% CO_2. Muscle samples were trimmed to 1-1.5 mm thick bundles in aerated saline parallel to the fiber long axis and fastened at each end using 5-0 surgical silk. Fiber bundles were then stretched and held at 110% of resting length by dental wax affixed to a wood

dowel (for fiber morphometry and TEM), or in a Petri dish containing aerated saline solution (for *ex vivo* stimulation-recovery experiments). For examining COX activity, white muscle was excised contralateral to that removed for the PCr experiments, frozen in cryo-tubes in liquid nitrogen, and stored at -80ºC until processed.

Fiber Size

For morphometric examination of *C. striata* epaxial white muscle, fiber bundles from the left side of the fish were blotted dry and frozen in isopentane (2-methylbutane; Fisher Scientific, Pittsburg, PA) cooled in a liquid nitrogen bath. Frozen samples were embedded in a pyramid of tragacanth gum (50 $g \cdot L^{-1}$; ICN Biomedicals, Inc., Aurora, OH) and mounted on a four cm^2 corkboard. The entire sample was inverted and submerged in the cooled isopentane until completely frozen (approximately 30-60 s depending on preparation size). Frozen tragacanth mounts were wrapped in parafilm to reduce desiccation and stored at -80 °C until sectioning.

Frozen mounts were acclimated to –19 °C for 20 min in a Reichert-Jeung Cryocut 1800 cryostat (Leica Microsystems Inc., Bannockburn, IL), sliced in 12 μm thick sections from an arbitrary starting point, and stained using Groat's variation for Weigert haemotoxylin stain (Groat, 1949) for 3-5 min followed staining in eosin for 60 s. Stained slides were viewed under an Olympus BX-60 microscope (Olympus America, Inc, Melville, NY) and digitized with a Diagnostic Instruments Spot RTke camera (Diagnostic Instruments, Sterling Heights, MI). Polygons of fibers were traced from the micrographs using the quick-mask feature in Adobe Photoshop v7.0. Cell diameters were determined using Image-Pro Plus (IPP) v4.1.0.9 software, which had been calibrated with a reticle at each magnification. IPP calculated the average diameter of the polygon traces through the centroid in 2-degree increments around the circumference of the cell.

Mitochondrial Distribution

Mitochondrial fractional volumes and distributions were examined using transmission electron microscopy (TEM). All six small fish and five of the six large fish used for this section were also used for fiber size. Muscle from the right side of the fish was excised, tied and stretched in the same manner described above. Preparations were fixed at room temperature in 2.5% glutaraldehyde with 0.2 M sodium cacodylate buffer (pH 7.4 and 300 mOsm) for at least 24 h, rinsed twice (15 min each) in cacodylate buffer, and placed in a secondary fixative of OsO_4 for 2 h. After another buffer rinse and two five min DI rinses, preparations were dehydrated in increasing concentrations of acetone (50, 70, 95, and twice at 100%) for 15 min each. Preparations were then infiltrated first with a 1:1 mixture of 100% acetone and 100% Spurr's epoxy resin (Spurr, 1969; Electron Microscopy Sciences, Hatfield, PA) for 1 h and then in 100% resin for at least 12 hours. Preparations were embedded in 100% resin hardened in a 70 °C oven for 8 h.

To analyze mitochondrial fractional volume, a systematic random sampling method (Howard and Reed, 1998) was applied in two separate sampling stages to ensure sufficient representation of mitochondrial distribution down the length of the muscle and across fiber area. Thin sections of embedded tissue were collected in 90 nm sections from an arbitrary starting point beginning at the anterior end of the muscle using glass knives on a Reichert-Jung Ultracut E (Leica Microsystems Inc., Bannockburn, IL). Five sections were collected on a Formvar-coated (0.25% Formvar in ethylene dichloride) high-transmission 200 mesh copper grid and then a distance of 500 nm was skipped before another five sections were collected. This process was repeated until a total of five grids were collected for each fish tissue. Grids were stained with 2% uranyl acetate in 50% ethanol and Reynolds' lead citrate (Reynolds, 1963). Sections were

examined on a Philips CM-12 STEM (Philips Research, Briarcliff Manor, NY) and micrographs were taken by the second application of a systematic random sampling method for each grid (Howard and Reed, 1998). This method was executed by magnifying the first section observed on a grid under low magnification 3000x, 5000x, or 8000x, after which the first 3 ¼" X 4" micrograph (referred to here as the field of view) was then taken and utilized as an arbitrary starting point for the two subsequent micrographs. The field of view was then moved across the magnified section by a distance equal to three times the field of view in any one direction. A second micrograph was collected at this new position and the process was repeated once more, for a total of three micrographs per grid (15 micrographs per tissue preparation). If any one position was severely obstructed by a grid bar, or was no longer on a section, a new field of view was sought in a direction 90° from the previous viable field of view. Micrographs were then developed and digitized using a Microtek Scanmaker 4 (Microtek Lab, Inc., Carson, CA).

Digitized micrographs were viewed in Adobe Photoshop v7.0 and a stereological point-counting method was applied to calculate mitochondrial fractional volume (Howard and Reed, 1998). The grid function included in the Photoshop program was overlaid on the images. All points touching extracellular space were subtracted from the total number of points per micrograph. Points that landed on mitochondria were tallied as either sub-sarcolemmal (SS) if the mitochondrion lay between the sarcolemmal membrane and the myofibers, or inter-myofibrillar (IM) if they were located among myofibers, regardless of proximity to the sarcolemmal membrane. The sums of either SS or IM points from all micrographs taken for each fish were divided by the sum of points hitting cellular space to determine fractional volume (FV). Total mitochondrial fractional volume (TMFV) was calculated as simply the sum of SS mitochondrial fractional volume (SSFV) and IM mitochondrial fractional volume (IMFV).

Cytochrome-c Oxidase Activity

COX activity was determined spectrophotometrically using an enzyme assay kit purchased from Sigma-Aldrich (St. Louis, MO). Frozen tissues were homogenized in a ten-fold dilution of ice-cold enzyme extraction buffer (50 mM imidazole, 50 mM KCl, and 0.5 mM dithiothreitol, pH 7.4) and sonicated on ice for three 10-s bursts with a Fisher Scientific 60 sonic dismembranator (Pittsburg, PA). Up to one ml of homogenate was centrifuged at 12,000 *g* for 15 min at 4 °C. Assays were performed on an Ultrospec 4000 spectrophotometer at 20 °C, maintained by an Isotemp 3016 recirculating water bath (Fisher Scientific, Pittsburg, PA). For each assay, 125 µl of sample supernatant (or 250 µl if the signal acquired using 125 µl of sample was too noisy) was combined with 825 µl (or 700 µm if 250 µl of sample was added) of assay buffer (10 mM Tris-HCl, 120 mM KCl, pH 7.0), and 100 µl of ice-cold enzyme dilution buffer (10 mM Tris-HCl, 250 mM sucrose, pH 7.0), before adding 50 µL of the 0.22 mM ferrocytochrome-c substrate, for a final volume of 1.1 mL. Constituents were mixed by inversion and immediately placed in the spectrophotometer. The absorbance was read in ten s intervals for five min at 550 nm. A blank containing 950 µL assay buffer, 100 µL enzyme dilution buffer, and 50 µL ferrocytochrome-c solution was run in the same manner. Enzyme activity ($U \cdot ml^{-1}$) was calculated according to the formula provided in the kit:

$$U \cdot ml^{-1} = (\Delta A \cdot min^{-1}_{sample} - \Delta A \cdot min^{-1}_{blank}) \cdot dilution \cdot 1.1 \cdot (vol \cdot 21.84)^{-1}$$

where dilution is the dilution factor of the homogenized tissue, vol is the amount of enzyme extract added (either 125 µl or 250 µl), and 21.84 is the extinction coefficient between ferrocytochrome-c and ferricytochrome-c at 550 nm.

Phosphocreatine Recovery

Muscle tissue was excised and prepared as described above and rigid plastic rings were

tied to the end of each trimmed bundle with 5-0 surgical silk. Fiber bundles were allowed to recover from dissection perturbation for at least 30 min for small fish or 45 min for medium and large fish before experimental use. The post-dissection recovery period was ascertained by systematically freeze-clamping (in aluminum tongs cooled in liquid nitrogen) multiple muscle preparations at 15 min intervals to determine how long after dissection the maximal baseline [PCr] was achieved. Similar post-dissection recovery has been described by other researchers who performed nearly identical procedures on muscle (Moon *et al.* 1991; Ken Rodnick personal communication).

After recovery from dissection perturbation, isolated muscle preparations were then suspended between glass hooks that were attached to the thin plastic rings. The lower hook was secured to the rigid frame of the stimulation/perfusion lab stand (Radnoti Glass Technologies, Inc., Monrovia, CA) and the upper hook, made from a thin glass fiber, connected the tissue to an isometric force transducer (Harvard Apparatus, South Natick, MA). Once suspended and stretched to 110% resting length, muscle preparations were submerged in a ten ml water-jacketed, glass chamber with built-in electrodes (Radnoti Glass Technologies, Inc., Monrovia, CA) containing aerated saline maintained at 20 °C by an Isotemp 3016S recirculating water bath (Fisher Scientific, Pittsburg, PA). The fiber bundle was then field-stimulated using a Grass S88 physiological stimulator (Astro-Med, Inc. West Warrick, RI) at 70Hz. Preliminary experiments indicated that 120 s of stimulation was necessary to deplete PCr in all size classes. The voltage signal from the force transducer was digitized using a Biopac MP100 data acquisition system and recorded on a PC using Acqknowledge v.3.5.7 software (Biopac Systems, Inc., Santa Barbara, CA). Following stimulation, fiber bundles were allowed to recover for 0, 5, 10, 15, or 30 min. Bundles were then freeze-clamped in liquid nitrogen cooled tongs, transferred to small tubes, and

stored temporarily (no more than a few hours) in liquid nitrogen until extraction. Unstimulated bundles were used to determine resting [PCr] and frozen in the same manner at the end of the post-dissection recovery period previously described.

Frozen samples from the *ex vivo* stimulation experiments were weighed and homogenized using a PowerGen 125 homogenizer (Fisher Scientific, Pittsburg, PA) in 6-15 volumes of chilled perchloric acid (1M perchloric acid, 1 mM EDTA) to yield a final volume of approximately one ml. Homogenates were then centrifuged at 16,000 *g* for 30 min at 4 °C. The supernatants were transferred to a new micro centrifuge tube and neutralized to pH 6.5-7.5 using three M KCO^-_3 containing 50 mM PIPES, allowed to sit for 10 min after neutralization, and then centrifuged again at 16,000 *g* for 15 min at 4 °C. The supernatant was collected and placed in individual five mm NMR tubes.

Relative concentrations of P_i and PCr in muscle extracts were determined using ^{31}P-NMR spectra collected at 162 MHz on a Bruker 400 MHz DMX spectrometer (Bruker Biospin Corporation, Billerica, MA). Spectra were collected using a 45° excitation pulse (2.5 μs) and a 0.6 s relaxation delay. Four hundred scans were collected for a total acquisition time of five min. A 0.5 Hz line broadening exponential multiplication was applied prior to Fourier transformation. The area under the P_i and PCr peak of each spectra was integrated using Xwin-NMR software and compared to the peak area of a known concentration of PCr, from which the [PCr] of each extract was calculated.

Analysis

One-way analysis of variance (ANOVA) was used to test for significant effects of size class, and where significant size effects were detected Tukey's HSD test was used for pairwise comparisons (Boyle *et al.* 2003). A two-way ANOVA was implemented to examine the

interaction between size class and time on PCr recovery (Johnson *et al.* 2004). All statistical tests were analyzed with JMP software version 7.0.2 (SAS Institute, Cary, NC). In all cases, $P<0.05$ were considered significant. The linear regression of COX activity and TMFV data were each calculated using Sigma Plot version 8.02 (SPSS Inc., Chicago, IL; Johnson *et al.* 2004).

RESULTS

Fish and Fiber Size

The present study used fish ranging in body mass from 1.5 to 4496 g and in total body length from 45 to 544 mm (Fig. 2; Table 1). This corresponds to a mass range of nearly 3000 fold and a 12-fold increase in length. Figure 3 demonstrates hypertrophic growth exhibited by epaxial white muscle in *C. striata* during ontogeny, leading to large fibers in adults. The fiber diameters ranged from 5.3 to 80.4 μm (348 fibers) in the small fish, 16.4 to 152.5 μm (245 fibers) in the medium fish, and 74.1 to 465.4 μm (239 fibers) in the large animals (Fig. 4A). The distribution of muscle fiber diameters noticeably broadened during growth. One-way ANOVA indicated a significant effect of size class on mean fiber diameter ($F=2.35$, d.f.=2, $P<0.001$) and pair-wise comparisons indicated that each size class was significantly different from the other two (Fig. 4B; Tukey's HSD, $P<0.05$). The mean diameter of the small and medium size class differed by only two-fold despite a nearly 32-fold difference in mean body mass, while the difference in mean fiber diameter was 3.5-fold between the medium and large size classes, which corresponded to a 45-fold difference in body mass.

Mitochondrial Distribution

Representative TEM micrographs showing mitochondrial distribution are presented in Fig. 5. Mitochondrial density scaled negatively with body mass and the total mitochondrial fractional volume (TMFV), was significantly higher in the small fish than the

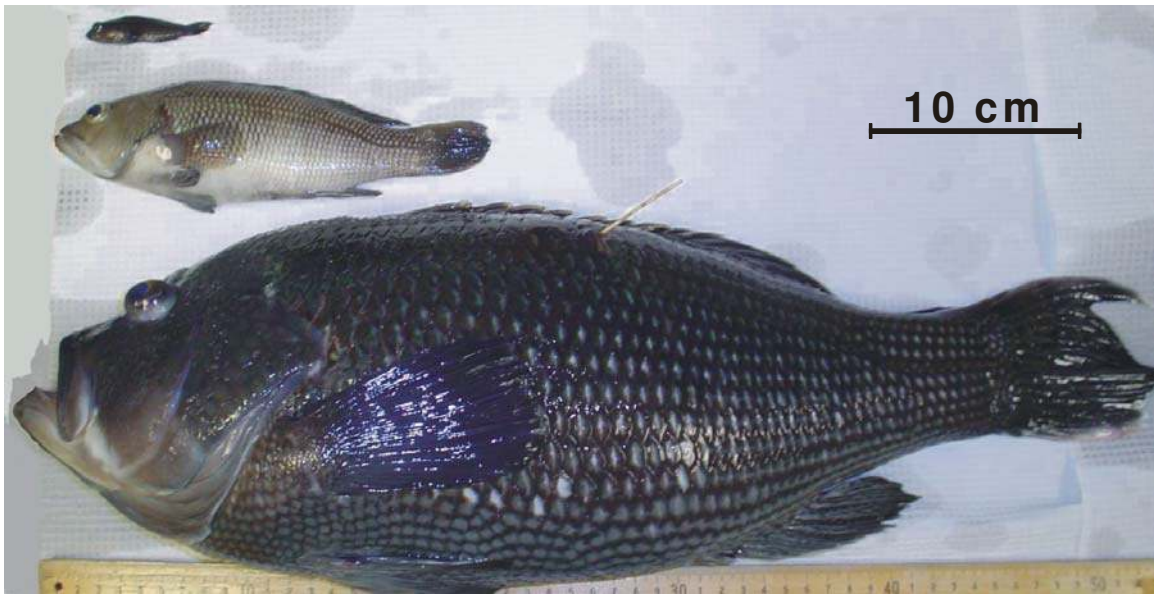

Figure 2. Representative individuals from each size class of *C. striata* used in the present study. The small (top) and medium (middle) size classes were reared by the UNCW Aquaculture Facility, while large fish (bottom) were wild-caught as adults and maintained as part of the facility's brood stock.

	Fiber Size			Mitochondrial Distribution			COX			Phosphocreatine Recovery		
Size Class	N	Mean body mass (g)	Body mass range (g)	N	Mean body mass (g)	Body mass range (g)	N	Mean body mass (g)	Body mass range (g)	N	Mean body mass (g)	Body mass range (g)
Small	7	2.40 ±0.76	1.5 – 5.8	6	1.85 ±0.17	1.5 – 2.2	12	6.22 ±1.07	1.6 – 14.2	24	11.11 ±0.76	5.7 – 20.8
Medium	7	77.01 ±2.32	46.7 – 181.8	--	--------	--------	15	87.88 ±11.15	43.5 – 196.9	12	401.52 ±55.70	56.6 – 765.1
Large	6	3531.47 ±60.33	2413.2 – 4496.5	6	3166.43 ±666.98	2413.2 – 4496.5	12	2332.08 ±297.11	948.5 – 3668.3	10	2507.93 ±315.85	948.5 – 4159.4

Table 1. Body size characteristics of fish and N values used for each type of experiment. N values represent number of fish in all experiments except mitochondrial distribution, in which case N represents the number of fixed fiber bundles (see Results for further explanation). In some cases, multiple strips of epaxial white muscle were isolated from a single fish and were used in multiple experiments. Values for mean body mass are mean ±SE.

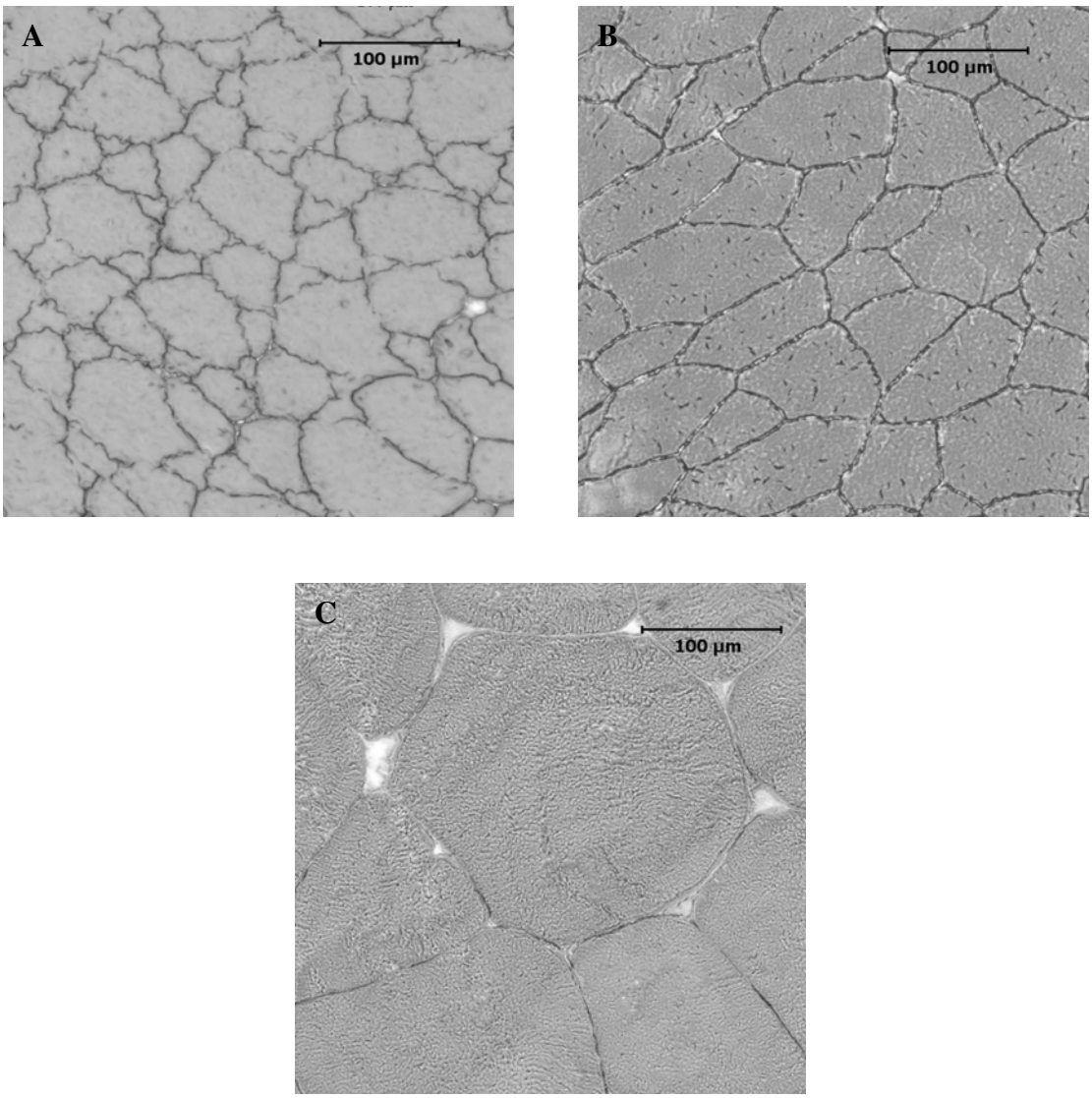

Figure 3. Representative cross-sections of *C. striata* white muscle fibers from small (A), medium (B), and large (C) fish at 20x magnification.

Figure 4. Distribution (A) and mean by size class (B) of epaxial white muscle cross-sectional fiber diameter from small, medium, and large fish. (A) The fiber cross-sectional diameters (μm), shown as percent frequency, are binned in 10 μm increments. (B) The * indicates that each size class is significantly different from the other two (Tukey's HSD, $P<0.05$). Values are means ±SEM.

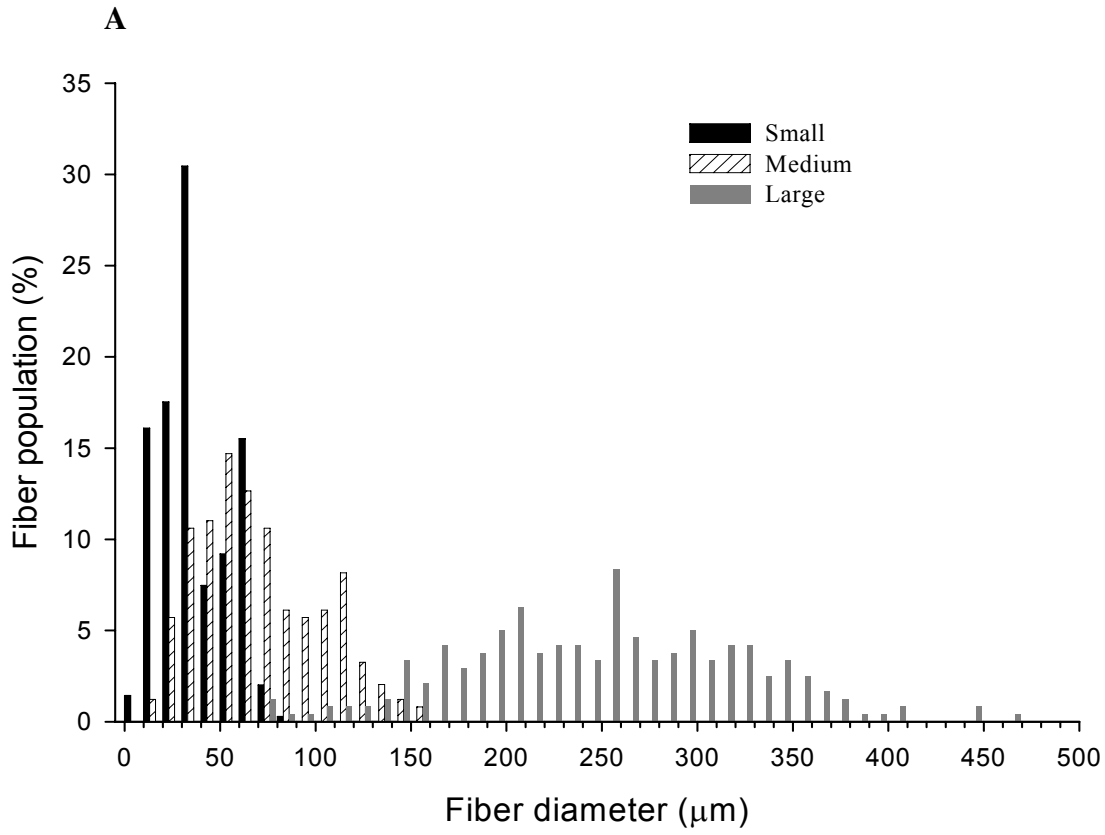
A
Small
Medium
Large
Fiber population (%)
Fiber diameter (μm)
0
5
10
15
20
25
30
35
0
50
100
150
200
250
300
350
400
450
500

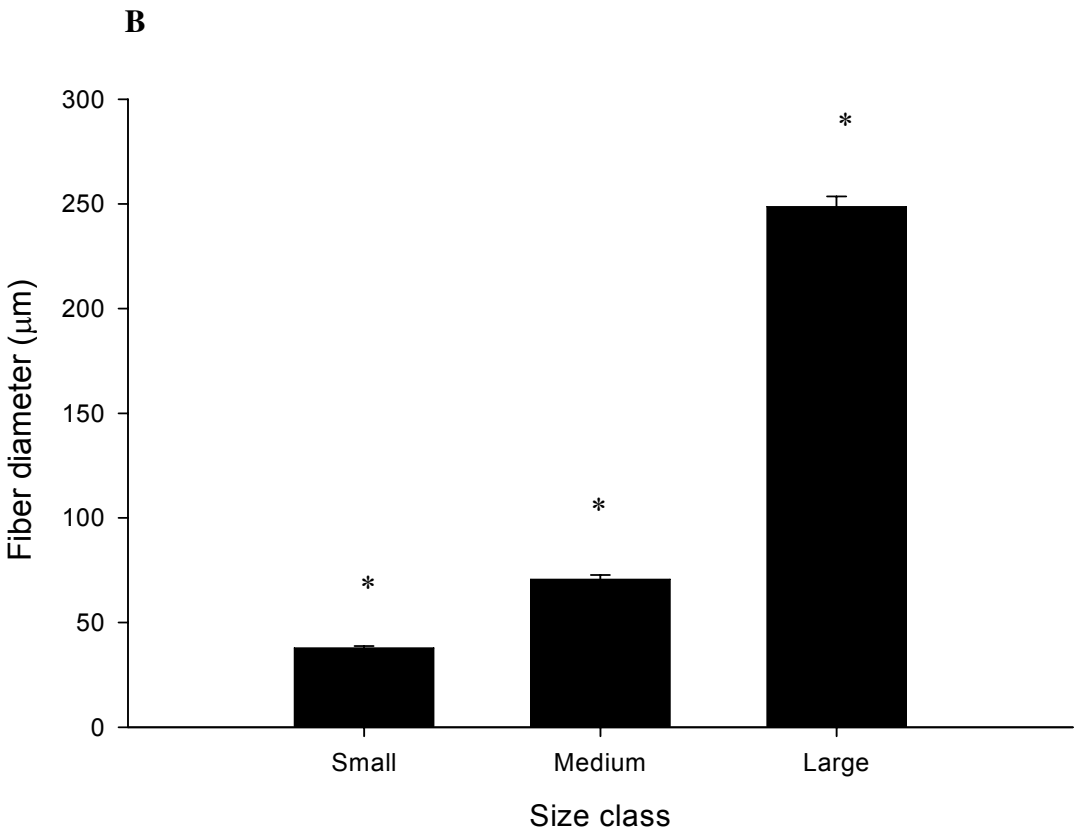
B
Fiber diameter (μm)
Size class
Small
Medium
Large
0
50
100
150
200
250
300
*
*
*

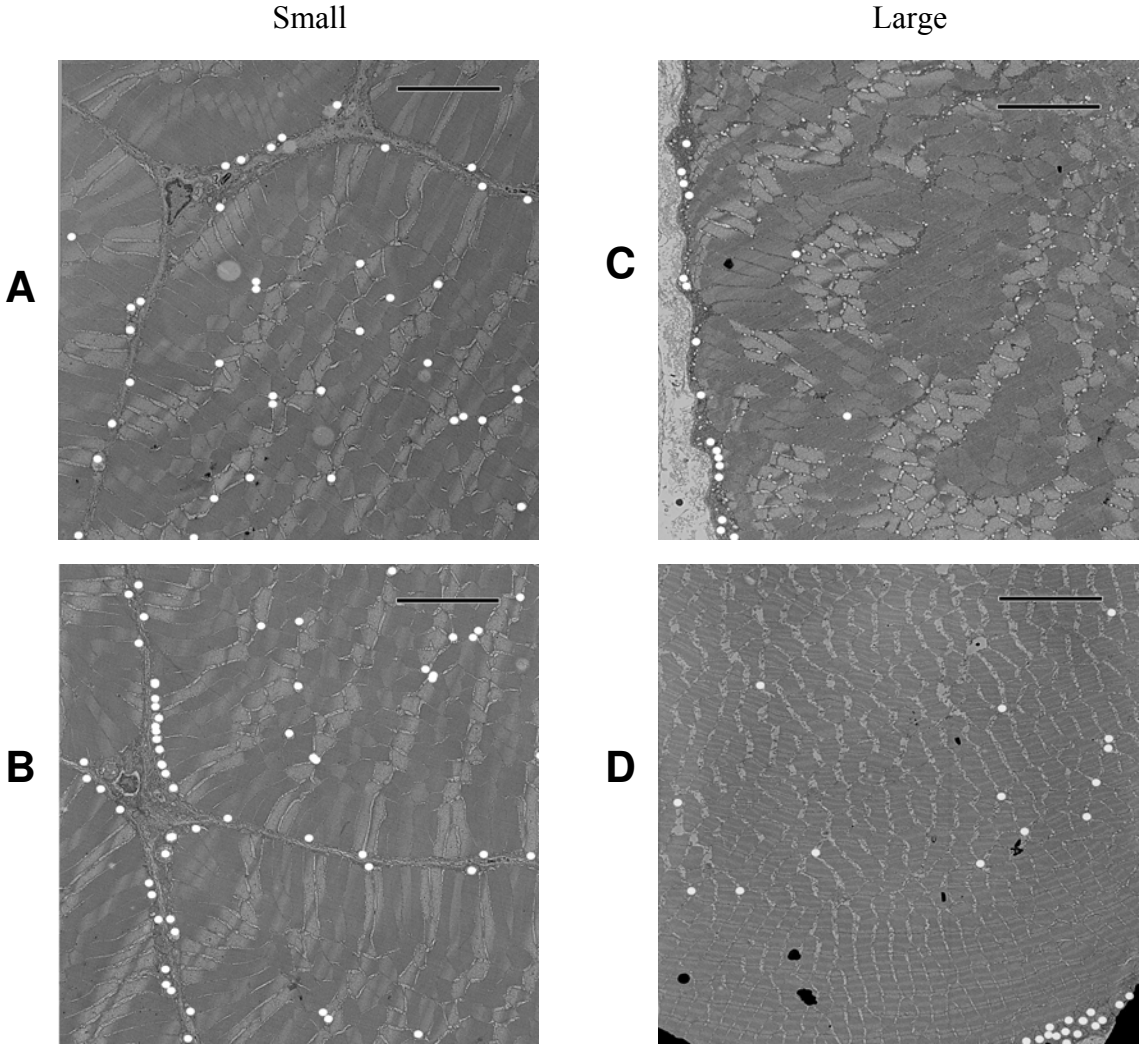

Figure 5. Examples of micrographs from small (left) and large (right) fish taken at a magnification of 3000x. The white dots mark the location of individual mitochondria. Both the sarcolemmal and the bulk of the intermyofibrillar spaces are visible in the two examples from the small size class fish (A & B). The fibers from the large size class were too large to show a comparable percentage of the cell, so panel C shows the SS mitochondria, while D shows typical densities of IM mitochondria and a small section of the sarcolemmal with part of a SS mitochondrial cluster in the lower right corner. Scale bar = 5 μm.

large (Fig. 6A; Tukey's HSD, $P<0.05$). Both inter-myofibrillar mitochondrial fractional volume (IMFV; Tukey's HSD, $P<0.05$) and sub-sarcolemmal mitochondrial fractional volume (SSFV; Tukey's HSD, $P<0.05$) decrease with increasing body mass, but there were no significant differences between size classes in either category (Fig. 6A). To determine whether SS were clustered more densely in large fibers than in small (Boyle *et al.* 2003), the SS mitochondrial volume per sarcolemmal membrane area (SSMV/SA) was calculated by dividing SSFV, ascertained by TEM, by the mean fiber SA:V, calculated from fiber size. Given that the same fish used in determining fiber diameter were also used to measure mitochondrial fractional volume, the SA:V could be accurately calculated. A significant increase in the SSMV per sarcolemmal membrane area was found (Fig. 6B; Tukey's HSD, $P<0.05$), indicating a greater clustering of mitochondria at the sarcolemmal membrane in the fibers of large fish.

Cytochrome-c Oxidase Activity

A line was fitted to the m ass specific COX activity according to the scaling relationship: COX activity = aM^b, where M is animal mass, a is a constant, and b is the scaling exponent (Schmidt-Nielsen, 1984). The COX activity of epaxial white muscle from 39 fish (Table 1) scaled negatively with body mass with a slope of -0.10 (Fig. 7; $r^2= 0.11$). This scaling exponent is similar to the value for TMFV of -0.06 obtained using the data in Fig. 6 (graph not shown).

Phosphocreatine Recovery

A typical trace of force production during intermittent stimulation in isolated muscle fiber bundles is presented in Fig. 8. Mean (± SEM) baseline values of [PCr] in $\mu M \cdot g^{-1}$ were 23.6 (±1.7), 20.2 (±1.3), and 17.3 (±1.5) in small, medium, and large, respectively, and each were significantly different from their respective post-contraction [PCr] (Fig. 9; Tukey's HSD, $P<0.05$). Aerobic recovery rate for all size classes was slow, and complete recovery required

Figure 6. The mitochondrial fractional volume (A) and sub-sarcolemmal mitochondria per membrane area (SSMV/SA; B). (A) Total mitochondrial fractional volume (TMFV; ●), sub-sarcolemmal mitochondrial fractional volume (SSFV; ▽), and intermyofibrillar mitochondrial fractional volume (IMFV; ■). The * indicates that only TMFV is significantly different between the two sizes (Tukey's HSD, $P < 0.05$). (B) The sub-sarcolemmal mitochondria volume per membrane area (SSMV/SA) in the small and large size classes. The * indicates that the means are significantly different (Tukey's HSD, $P < 0.05$). Values shown are means ± SEM.

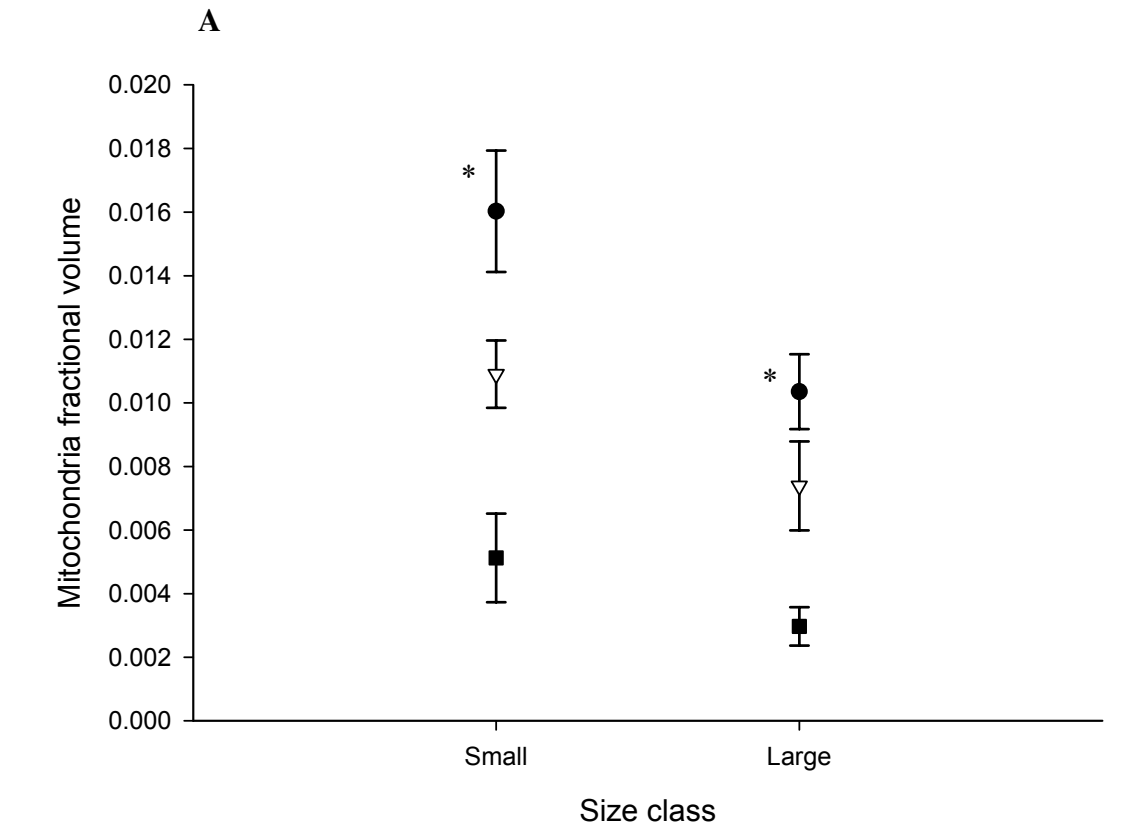
A
Mitochondria fractional volume
0.020
0.018
0.016
0.014
0.012
0.010
0.008
0.006
0.004
0.002
0.000
*
*
Small
Large
Size class

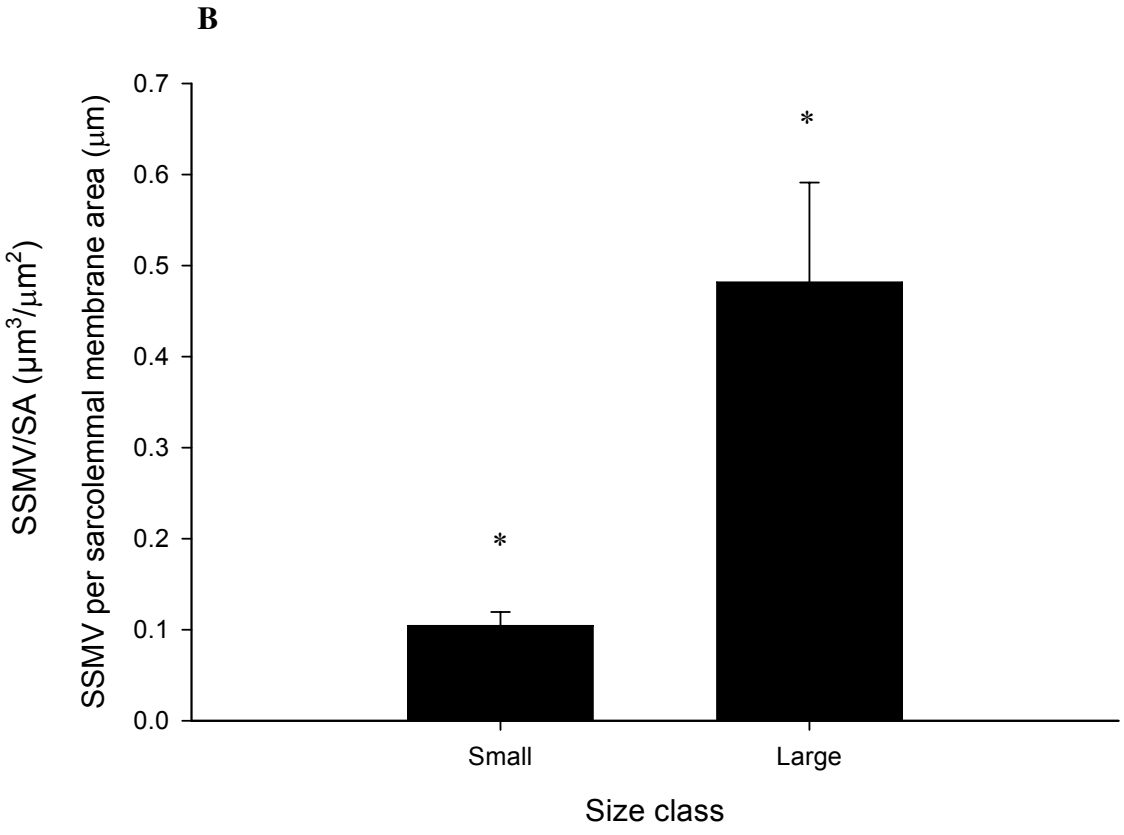
B
SSMV per sarcolemmal membrane area (μm)
SSMV/SA (μm³/μm²)
0.7
0.6
0.5
0.4
0.3
0.2
0.1
0.0
*
*
Small
Large
Size class

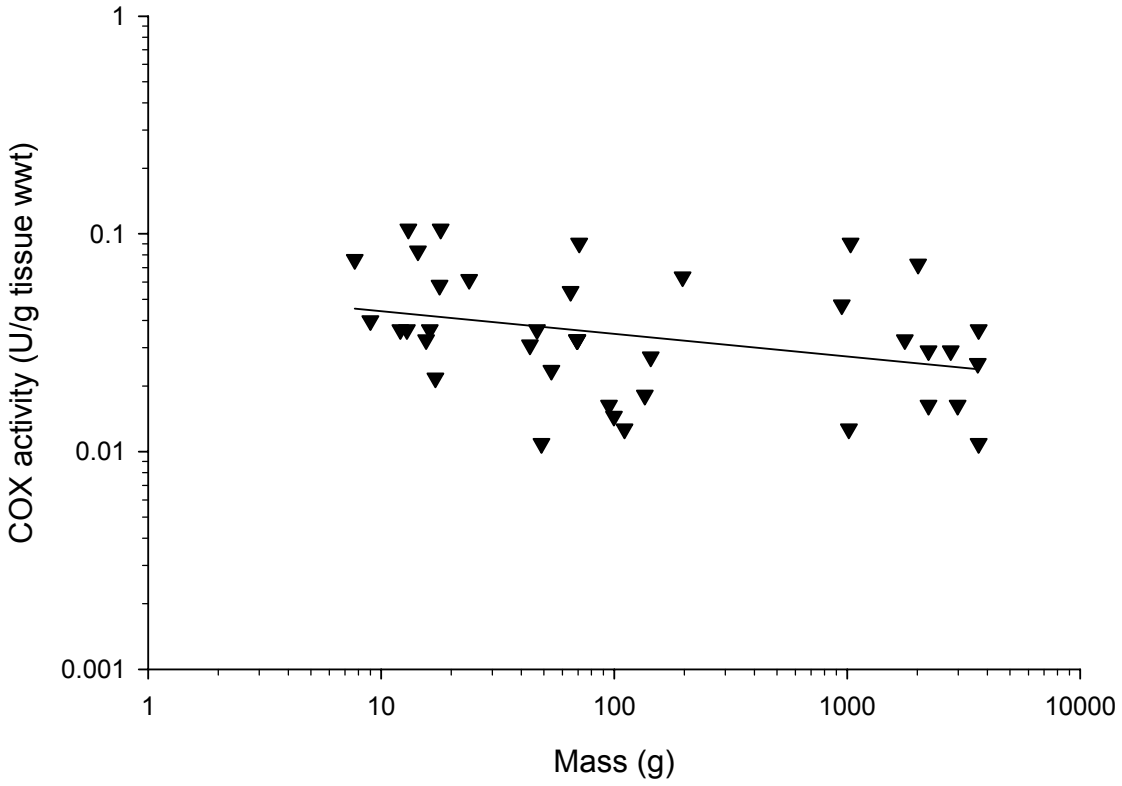

Figure 7. Scaling with body mass of cytochrome-*c* oxidase activity from epaxial white muscle of *C. striata*. The slope of the line is b = -0.10 (see text; $r^2 = 0.11$)

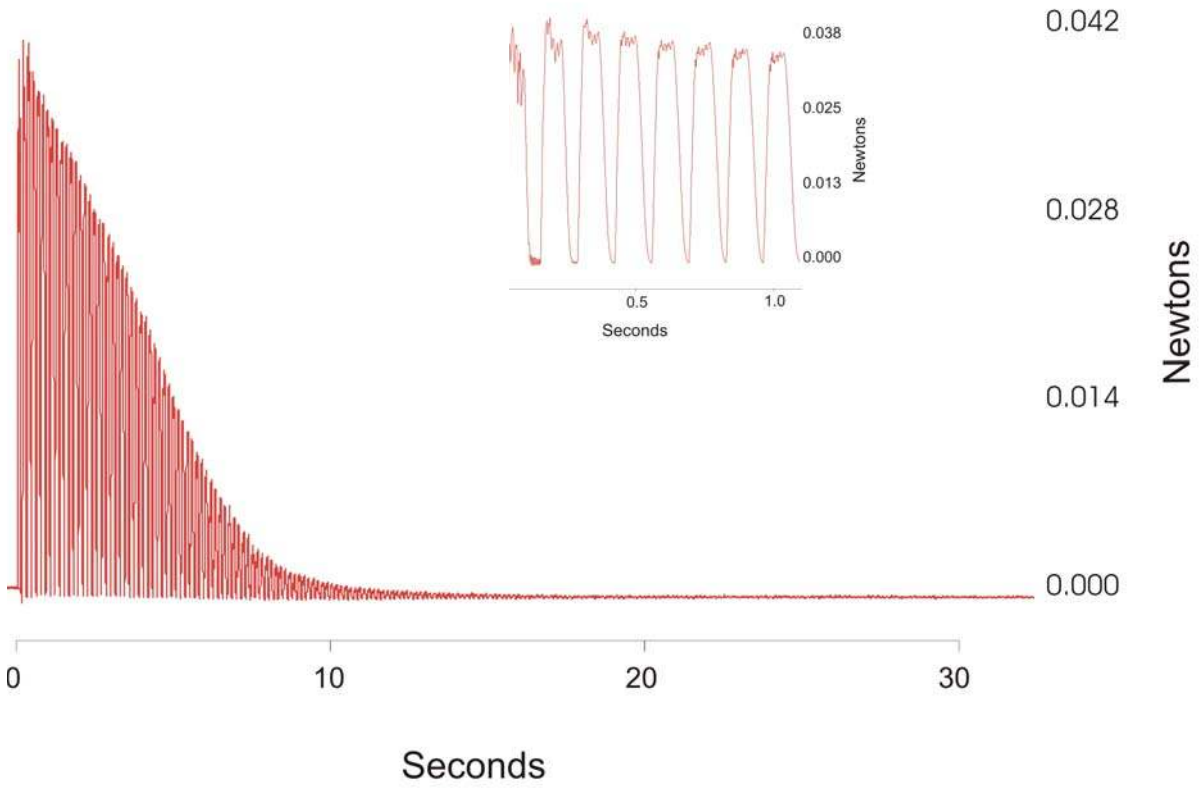

Figure 8. An example of the first 30 s of stimulation of an isolated muscle preparation from a small fish. The inset depicts the first second of contractions from the larger plot.

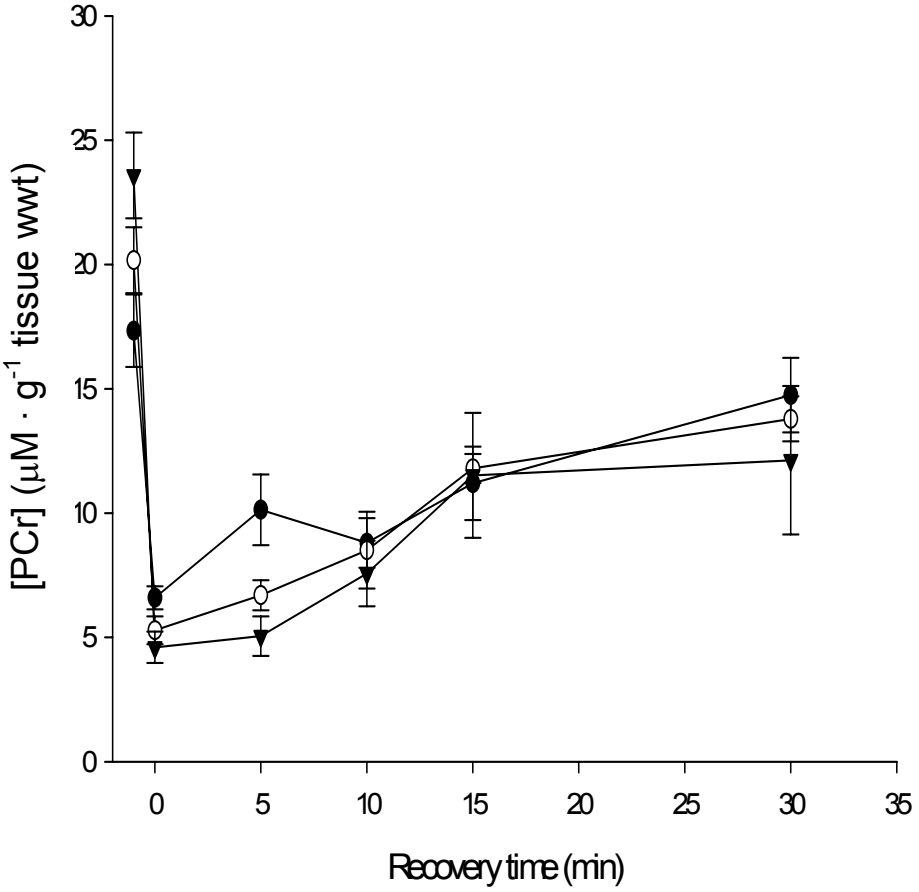

Figure 9. The phosphocreatine recovery over 30 minutes between small (▼), medium (○), and large (●) size classes. Each time point within each size has n ≥ 5 replicates and values shown are means ± SEM.

more than one hour for all size classes. However, due to increased variation in muscle fiber viability over this prolonged recovery period, the present study used data for the initial 30 min only. Two-way ANOVA showed that there was no significant interaction of size class on recovery time (Fig. 9; F=1.399, d.f.=10, P=0.189).

DISCUSSION

The major findings of the present study were (1) hypertrophic growth of white muscle fibers occurred during ontogeny, and this growth is associated with negative scaling of both mitochondrial density and COX activity, (2) a significant increase in the amount of sarcolemmal membrane occupied by mitochondria occurs during fiber growth, (3) the rate of PCr recovery was independent of fish body mass (and therefore fiber size), and (4) the rate of post-contractile recovery of PCr was too slow to be limited by intracellular metabolite diffusion, based on a comparison to the reaction-diffusion analysis of Kinsey *et al.*(2005).

Skeletal muscle in fish is often partitioned into discrete regions of red (oxidative) and white (glycolytic) fibers (e.g. Gill *et al.* 1989). White muscle fibers are typically characterized as having lower oxidative capacity and larger diameters relative to the other types of fish skeletal muscle (Kryvi *et al.* 1980; Martinez *et al.* 2000), and there are examples of white fibers attaining very large dimensions (Weatherly and Gill, 1985; Fernandez *et al.* 2000; Johnston *et al.* 2003). However, the white muscle fibers in many fish species do not grow to particularly large sizes (Weatherly and Gill, 1985; Onali *et al.*1996; Martinez *et al.* 2000). For example, species such as carp (*Cyprinus carpio*; Koumans *et al.* 1993) and white sea bass (*Atractoscion nobilis*; Zimmerman *et al.* 1999), which attain body masses as adults that are similar to, or greater than, the adult *C. striata* used in this study, exhibit much smaller mean white muscle fiber diameters. The adult *C. striata* we utilized were wild-caught fish that were utilized for brood stock at the

UNCW Aquaculture Facility. Thus, the large fiber diameters observed in the adult *C. striata* in this study (Fig. 4B) are not likely to be related to captivity. The possible implications of decreased SA:V and increased diffusion distances on aerobic metabolism due to hypertrophic muscle growth makes the muscle fibers of these fish an interesting model system.

The TMFV (Fig. 6A) was within the range reported in white muscle of other temperate fish species (Kryvi *et al.* 1980; Walesby and Johnston, 1980; Egginton and Sidell, 1989). Also, the negative scaling exponent of COX activity (b = -0.10) corresponds fairly well with that of TMFV (b = -0.06). The finding that SSFV was greater than IMFV in both size classes was interesting. Given the small fiber diameters, the white fibers of small fish were anticipated to exhibit a more uniform mitochondrial distribution throughout the muscle fibers (Boyle *et al.* 2003). Low rates of O_2 supply to the muscle due to sparse vascularization, which is typical of teleost white muscle (Kryvi *et al.* 1980; Egginton and Sidell, 1989), is a possible reason for the predominance of sub-sarcolemmal mitochondria observed in all sizes of *C. striata*. That is, mitochondria may be distributed at the sarcolemmal membrane to be close to the source of O_2 in the fiber irrespective of body size. The significant increase in the amount of sarcolemmal membrane occupied by mitochondrial volume in large *C. striata* (Fig. 6B) may help counteract the additional challenge of a low SA:V in the large fibers. This finding is similar to, although less dramatic than, the shift in mitochondria observed during hypertrophic growth in the large white fibers of *C. sapidus*, which was attributed to low fiber SA: V (Boyle *et al.* 2003; Kinsey *et al.* 2005). Mainwood and Rakusan (1982) showed mathematically that by distributing mitochondria near the capillaries (i.e. peripheral distribution) the intracellular O_2 gradient across the fiber was considerably less steep than when mitochondria were evenly distributed over the entire fiber, even in relatively small fibers. Furthermore, they indicated that the presence of a

phosphagen kinase (e.g., CK) helped maintain a more uniform concentration of ATP across the cellular space. In both adult *C. striata* and adult *C. sapidus* the predominantly sub-sarcolemmal mitochondrial distribution may help offset the effects of low SA:V, but it also leads to increased intracellular diffusion distances between mitochondrial clusters and sites of ATP utilization, which may constrain rates of aerobic metabolism (Kinsey *et al.* 1999; Kinsey and Moerland, 2002; Boyle *et al.* 2003).

Muscle contraction is an anaerobic process and therefore not affected by the low SA:V or potentially long intracellular diffusion distances that typify large fibers. Post-contractile PCr recovery, however, is powered exclusively by aerobic metabolism in fish white muscle (Curtin *et al*. 1997). Kinsey *et al.* (2005) analyzed *in vivo* post-contractile recovery rates of AP in the white swimming muscle of *C. sapidus* using a mathematical reaction-diffusion model of aerobic metabolism. They concluded that diffusion did not limit aerobic AP recovery in large fibers, and suggested that SA:V exerted more influence over metabolic fluxes and intracellular characteristics. The present study used superfused muscle fiber preparations in a solution with high PO_2, which maximized the oxygen gradient across the fiber bundle and, thus, removed the effect of SA:V on metabolic recovery. This approach allowed an examination of the effect of intracellular metabolite diffusion on PCr recovery in isolation, without the confounding effects of fiber-size dependent limitations on O_2 flux as in previous work (Boyle *et al*. 2003; Johnson *et al*. 2004; Kinsey *et al*. 2005). PCr recovered slowly in all size classes, and was incomplete 30 min after contraction. Furthermore, there was no significant interaction between size class and recovery time on post-contractile PCr concentration, indicating that recovery rate did not differ significantly among size classes (Fig. 9). The rate of PCr recovery observed in the present study is comparable to that found in isolated white muscle from dogfish, *Scyliorhinus canicula* (Curtin

et al. 1997), and to *in vivo* rates of recovery in white muscle of rainbow trout, *Oncorhynus mykiss* (Schulte *et al.* 1992), tilapia, *Oreochromis mossambicus*, (Van Ginneken *et al.* 1999), and Pacific spiny dogfish, *Squalus acanthias* (Richards *et al.* 2003). Additionally, the observed rates are similar to that of AP recovery in *C. sapidus* white fibers (Kinsey *et al.* 2005), which have similar fiber dimensions and mitochondrial content to *C. striata*. The size class independence of PCr recovery in *C. striata* occurred despite significant differences in fiber diameter and mitochondrial organization, suggesting that the large fibers are not limited by intracellular metabolite diffusion. This conclusion is further supported by the reaction-diffusion mathematical analysis conducted by Kinsey *et al.* (2005), which demonstrated that a rate comparable to that observed for the PCr recovery rate observed in the present study was too slow to be substantially limited by intracellular metabolite diffusion, and underscores their hypothesis that SA:V exerts more control over cellular organization and aerobic process rates.

The fact that small fish did not recovery more rapidly than the other size classes is interesting considering the higher SA:V, TMFV and COX activity of the fibers from the small fish, compared to those in the large fish. It is conceivable that PCr recovery in *C. striata* may be slow in all size classes due to inhibition of the CK reaction or glycolysis by low pH following contraction (reviewed in McMahon and Jenkins, 2002). Alternatively, fibers from large fish may employ other strategies to expedite recovery, such as using anaerobic glycolysis to speed up PCr resynthesis. Post-contractile lactate accumulation is common in crustacean white muscle fibers from adult animals (Head and Baldwin, 1986; Henry *et al.* 1994; Milligan *et al.* 1989), and Johnson *et al.* (2004) first demonstrated that lactate accumulation was fiber size dependent, occurring only in the largest fibers. However, PCr resynthesis following contraction in vertebrates is exclusively aerobic (Kushmerick, 1983; Meyer, 1988; McMahon and Jenkins,

2002), including in isolated fish white muscle (Curtin *et al.* 1997). Although lactate concentration was not measured in the present study, the evidence from prior studies suggests that recovery of PCr in *C. striata* muscle is aerobic.

It could be argued that the use of isolated tissue or the *ex vivo* stimulation protocol may have detrimentally affected muscle metabolism. For instance, the resting (pre-contraction) PCr concentrations were lower in larger size class fish (Fig. 9). The need to maintain a small muscle preparation size across all fish size classes to allow for sufficient O_2 diffusion into the fiber core meant that there were always more fibers in excised bundles from small fish than in large fish. Therefore, the inverse relationship between resting [PCr] and size is likely an artifact of the higher proportion of severed fibers in preparations from large fish than smaller. However, baseline [PCr] values reported here are in good agreement with *in vivo* values reported in white muscle of *O. mykiss*, (Schulte *et al.* 1992; Hochachka and Mossey, 1998) and *S. acanthias*, (Richards *et al.* 2003), and are also similar to values from isolated white muscle from *S. canicula* (Curtin *et al.* 1997). Further, the similar rates of PCr recovery observed here to prior studies in fish muscle, conducted using a diversity of methods (Schulte *et al.* 1992; Curtin *et al.* 1997; Richards *et al.* 2003), suggests that the approach employed in the present study is an effective means of assessing metabolic recovery.

In fish that undergo a large increase in body mass, prolonged muscle hypertrophy leading to large fibers in adults may be the default developmental strategy if there are no selective pressures against large fiber size. Although the experimental approach used here eliminated the effects of SA:V on PCr recovery, the expectation is that the low SA:V of the large fibers would lead to a slowed rate of PCr recovery *in vivo* in the large fish. In the wild, the slow rate of PCr recovery would mean that bouts of high power contractions would be followed by a relatively

protracted recovery period before a similar bout of contractions could occur. The fish in this study had no discernable medial-lateral red muscle, which has been observed in other fish (Goolish, 1991). The lack of medial-lateral red muscle in *C. striata* suggests that swimming at higher speeds is powered almost exclusively by white muscle, whereas routine locomotion is slow and relies largely on labriform swimming (personal observations). Black sea bass therefore appear to be capable of extended periods of very slow aerobic swimming, or short bursts of high velocity swimming, but they are not well equipped for sustained periods of swimming at intermediate velocities. Since *C. striata* is a benthic fish associated with hard bottom communities, and is often in close proximity to cover, a protracted recovery following burst swimming may not have negative consequences. That is, aspects of the animal's behavior may make large fiber size a relatively unimportant constraint.

It is also possible that there is positive selection for the presence of large fibers in fish white muscle. Johnston *et al*. (2004) proposed that the cost of maintaining cellular ion balance is relatively high, and since a large amount of the body mass in most teleosts is white muscle, ion homeostasis within this tissue contributes considerably to whole animal metabolism. Additionally, they state that the lowered SA:V in tissues comprised of large cells would lead to less membrane leak, and therefore fewer ion pumps would be required to maintain ion balance. At present, however, it is unclear whether large cells arise as a natural consequence of hypertrophic growth in species with a large body mass range and behavioral patterns that obviate the need for rapid metabolic recovery, or whether there is selection in favor of large cells in order to lower energetic costs associated with ion homeostasis.

In summary, this study characterized the epaxial white musculature in *C. striata* and investigated the effects of hypertrophy on post-contractile PCr recovery, which is the product of

an aerobic process. *C. striata* white muscle fiber diameters become very large during ontogeny, and the proportion of the sarcolemmal membrane occupied by mitochondria is significantly greater in large fibers than in small fibers. PCr recovery was found to be independent of body mass and fiber size despite the extreme dimensions attained during hypertrophic white muscle growth, and the rate of PCr recovery was too slow to be limited by intracellular metabolite diffusion. It is therefore likely that low mitochondrial density is primarily responsible for the slow rate of PCr recovery, and fiber SA:V is a more important factor than intracellular metabolite flux on metabolic design in fish white muscle fibers that attain large sizes.

LITERATURE CITED

Battram, J.C. and Johnston, I.A. (1991). Muscle growth in the Antarctic teleost, *Notothenia neglecta* (Nybelin). *Antarctic Science* **3**, 29-33

Boyle, K-L., Dillaman, R.M. and Kinsey, S.T. (2003). Mitochondrial distribution and glycogen dynamics suggest diffusion constraints in muscle fibers of the blue crab *Callinectes sapidus*. *J. Exp. Zool.* **297A**, 1-16.

Childress, J.J. and Somero, G.N. (1990). Metabolic scaling: a new perspective based on scaling of glycolytic enzyme activies. *Amer. Zool.* **30**, 161-173.

Curtin, N.A., Kushmerick, M.J., Wiseman, R.W. and Woledge, R.C. (1997). Recovery after contraction of white muscle fibers from the dogfish *Scyliorhinus canicula*. *J. Exp. Biol.* **200**, 1061-1071.

Dobson, G.P. and Hochachka, P.W. (1987). Role of glycolysis in adenylate depletion and repletion during work and recovery in teleost white muscle. *J. Exp. Biol.* **129**, 125-140.

Ellington, W. R. and Kinsey, S. T. (1998). Functional and evolutionary implications of the distribution of phosphagens in primitive-type spermatozoa. *Biol. Bull.* **195**, 264-272.

Egginton, S. and Sidell, B.D. (1989). Thermal acclimation induces adaptive changes in subcellular structure of fish skeletal muscle. *Am. J. Physiol.* **256**, R1-R9.

Fernandez, D.A., Calvo, J., Franklin, C.E. and Johnston, I.A. (2000). Muscle fibre types and size distribution in sub-antarctic notothenioid fishes. *J. Fish Biol.* **56**, 1295-1311.

Gill, H.S., Weatherly, A.H., Lee, R. and Legere, D. (1989). Histochemical characterization of mytomal muscle of five teleost species. *J. Fish Biol.* **34**, 375-386.

Goolish, E.M. (1991). Aerobic and anaerobic scaling in fish. *Biol. Rev.* **66**, 33-56.

Groat (1949). Initial and persisting staining power of solutions of iron haemotoxylin lake. *Stain Tech.* **24**,157-163. In: *Humason's Animal Tissue Techniques 5th ed*. Presnell, J.K. and Schreibman, M.P. Johns Hopkin's Univ. Press, Baltimore. 1997, p. 103.

Head, G. and Baldwin, J. (1986). Energy metabolism and the fate of lactate during recovery from exercise in the Australian freshwater crayfish, *Cherax destructor. Aust. J. Mar. Freshwater Res.* **37**, 641-646.

Henry, R.P., Booth, C.E., Lallier, F.H. and Walsh, P.J. (1994). Post-exercise lactate production and metabolism in three species of aquatic and terrestrial decapod crustaceans. *J. Exp. Biol.* **186**, 215-234.

Hochachka, P.W. and Mossey, M.K. (1998). Does muscle creatine phosphokinase have access to the total pool of phosphocreatine plus creatine? *Am. J. Physiol.* **274**, R868-R872.

Howard, C.V. and Reed, M.G. (1998). *Unbiased Stereology, 3-Dimensional Measurements in Microscopy.* Oxford: BIOS Scientific Publishers.

Hubley, M.J., Locke, B.R. and Moerland, T.S. (1997). Reaction-diffusion analysis of the effects of temperature on high-energy phosphate dynamics in goldfish skeletal muscle. *J. Exp. Biol.* **200**, 975-988.

Jacobson, K.A. and Wojcieszyn, J.W. (1984). The translational mobility of substances within the cytoplasmic matrix. *Proc. Natl. Acad. Sci. USA* **81**, 6747-6751.

Johnson, L.K., Dillaman, R.M., Gay, D.M., Blum, J.E. and Kinsey, S.T. (2004). Metabolic influences of fiber size in aerobic and anaerobic locomotor muscles of the blue crab, *Callinectes sapidus. J. Exp. Biol.* **207**, 4045-4056.

Johnston, I.A., Fern*á*ndez, D.A., Calvo, J., Vieira, V.L.A., North, A.W., Abercromby, M. and Garland, T. (2003). Reduction in muscle fibre number during the adaptive radiation of notothenioid fishes: a phylogenetic perspective. *J. Exp. Biol.* **206**, 2595-2609.

Johnston, I.A., Abercromby, M., Vieira, V.L.A., Sigursteindóttir, R.J., Kristjánsson, B.K., Sibthorpe, D. and Skúlason, S. (2004). Rapid evolution of muscle fibre number in post-glacial populations of Arctic charr *Salvlinus aplinus*. *J. Exp. Biol.* **207**, 4343-4360.

Kay, L., Li, Z., Mericskay, M., Olivares, J., Tranqui, L., Fontaine, E., Tiivel, T., Sikk, P., Kaambre, T., Samuel, J-L., Rappaport, L., Usson, Y., Leverve, X., Paulin, D. and Saks, V.A. (1997). Study of regulation of mitochondrial respiration in vivo. An analysis of influence of ADP diffusion and possible role of cytoskeleton. *Biochimica et Biophysica Acta* **1322**, 41-59.

Kinsey, S.T., Locke, B.R., Penke, B. and Moerland, T.S. (1999). Diffusional anisotropy is induced by subcellular barriers in skeletal muscle. *NMR Biomed.* **12**, 1-7.

Kinsey, S.T. and Moerland, T.S. (2002). Metabolic diffusion in giant muscle fibers of the spiny lobster *Panulirus argus*. *J. Exp. Biol.* **205**, 3377-3386.

Kinsey, S.T., Pathi, P., Hardy, K.A., Jordan, A. and Locke, B.R. (2005). Does intracellular metabolite diffusion limit post-contractile recovery in burst locomotor muscle? *J. Exp. Biol.* **208**, 2641-2652.

Koumans, J.T.M., Akster, H.A., Booms, G.H.R. and Osse, J.W.M. (1993). Growth of carp (*Cyprinus carpio*) white axial muscle; hyperplasia and hypertrophy in relation to the myonucleus/sarcoplasm ratio and the occurrence of different subclasses of myogenic cells. *J. Fish Biol.* **43**, 69-80.

Koumans, J.T.M. and Akster, H.A. (1995). Myogenic cells in development and growth of fish. *Comp. Biochem. Physiol.* **110A**(1), 3-20.

Kryvi, H., Flood, P.R. and Gulyaev, D. (1980). The ultrastructure and vascular supply of the different fibre types in the axial muscle of the sturgeon *Acipenser stellatus*, Pallas. *Cell Tissue Res.* **212**, 117-126.

Kushmerick, M.J. (1983). Energetics of muscle contraction. In *Handbook of Physiology,* Section 10, *Skeletal Muscle* (ed E.W. Taylor, S. Egginton, and J.A. Raven), pp. 45-67. Cambridge: Cambridge University Press.

Kushmerick, M.J. (1998). Energy balance in muscle activity: Simulations of ATPase coupled to oxidative phosphorylation and to creatine kinase. *Comp. Biochem. and Physiol.* **120B**, 109-123.

Lindstedt, S.L., McGlothlin, T., Percy, E. and Pifer, J. (1998). Task-specific design of skeletal muscle: balancing muscle structural composition. *Comp. Biochem. Physiol.* **120**, B35-B40.

Mainwood, G.W. and Rakusan, K. (1982). A model for inctracellular energy transport. *Can. J. Physiol.* **60**, 98-102.

Martínez, I.I., Cano, F.G., Zarzosa, G.R., Vázquez, J.M., Latorre, R., Albors, O.L., Arencibia, A. and Orenes, Y.M. (2000). Histochemical and morphometric aspects of the lateral musculature of difference species of teleost marine fish of the Percomorphi order. *Anat. Histol. Embryol.* **29**, 211-219.

McMahon, S. and Jenkins, D. (2002). Factors affecting the rate of phosphocreatine resynthesis following intense exercise. *Sports Med.* **32**(12), 761-784.

Meyer, R.A., Sweeney, H.L. and Kushmerick, M.J. (1984). A simple analysis of the 'phocphocreatine shuttle.' *Am. J.Physiol.* **246**, C365-C377.

Meyer, R. A. (1988). A linear model of muscle respiration explains monoexponential phosphocreatine changes. *Am. J. Physiol Cell Physiol.* **254**, 548-553.

Meyer, R. A. (1989). Linear dependence of muscle phosphocreatine kinetics on total creatine content. *Am. J. Physiol Cell Physiol.* **257**, 1149-1157.

Milligan, C.L., Walsh, P.J., Booth, C.E. and McDonald, D.L. (1989). Intracellular acid-base regulation during recovery from locomotor activity in the blue crab, *Callinectes sapidus. Physiol. Zool.* **62**, 621-638.

Moerland, T.S. and Egginton, S. (1998). Intracellular pH of muscle and temperature: insight from *in vivo* ^{31}P NMR measurements in a stenothermal Antarctic teleost (*Harpagifer antarcticus*). *J. Therm. Biol.* ***23***(5), 275-282.

Mommsen, T.P. (2001). Paradigms of growth in fish. *Comp. Biochem. Physiol.* **129B**, 207-219.

Moon, T.W., Altringham, J.D. and Johnston, I.A. (1991). Energetics and power output of isolated fish fast muscle fibres performing oscillatory work. *J. Exp. Biol.* **158**, 261-273.

Norton, S.F., Eppley, Z.A. and Sidell, B.D. (2000). Allometric Scaling of maximal enzyme activities in the axial musculature of striped bass *Morone saxatilis* (Walbaum). *Physiol. Biochem. Zool.* **73**(6), 819-828.

Onali, A., Ferri, A., Altavista, P.L., Colombari, P.T. and Alfei, L. (1996). Different contribution of hyperplasia and hypertrophy to the growth of common carp (*Cyprinus carpio* L.) cervical and caudal myotomal white muscle. *Anim. Biol.* **1**, 3-9.

Reynolds, E.S. (1963). The use of lead citrate at high pH as an electron opaque stain in electron microscopy. *J. Cell Biol.* **17**, 208-212.

Richards, J.G., Heigenhauser, G.J.F. and Wood, C.M. (2000). Exercise and recovery metabolism in the pacific spiny dogfish (*Squalus acanthias*). *J. Comp. Physiol.* **173B**, 463-474.

Russell, B., Motlagh, D. and Ashley, W.W. (2000). Form follows function: how muscle shape is regulated by work. *J. Appl. Physiol.* **88**, 1127-1132.

Schmidt-Nielsen, K. (1984). *Scaling: Why is Animal Size so Important?* Cambridge: Cambridge University Press.

Schulte, P.M., Moyes, C.D. and Hochachka, P.W. (1992). Integrating metabolic pathways in post-exercise recovery of white muscle. *J. Exp. Biol.* **166**, 181-195.

Somero, G.M. and Childress, J.J. (1980). A violation of the metabolism-size scaling paradigm: Activities of glycolytic enzymes in muscle increase in larger-size fish. *Physiol. Zool.* **53**(3), 322-337.

Somero, G.M. and Childress, J.J. (1990). Scaling of ATP-supplying enzymes, myofibrillar proteins and buffering capacity in fish muscle: relationship to locomotory habit. *J. Exp. Biol.* **149**, 319-333.

Spurr, R.A. (1969). A low-viscosity epoxy resin embedding medium for electron microscopy. *J. Ultractruct. Res.* **26**, 31-43.

Suarez, R.K. (2003). Shaken and stirred: muscle structure and metabolism. *J. Exp. Biol.* **206**, 2021-2029.

Tse F.W., Govind, C.K. and Atwood, H.L. (1983). Diverse fiber composition of swimming muscles in the blue crab, *Callinectes sapidus*. *Can. J. Zool.* **61**, 52-59.

Valente, L.M.P., Rocha, E., Gomes, E.F.S., Silva, M.W., Oliveira, M.H., Monteiro, R.A.F. and Fauconneau, B. (1999). Growth dynamics of white and red muscle fibres in fast- and slow-growing strains of rainbow trout. *J. Fish Biol.* **55**, 675-691.

Van Ginneken, V.J.T., Van Den Thillart, G.E.E.J.M., Muller, H.J., Van Deursen, S., Onderwater, M., Visée, J., Hopmans, V., Van Vliet, G. and Nicolay, K. (1999). Phosphorylation state of red and white muscle in tilapia during graded hypoxia: an in vivo ^{31}P-NMR study. *Am. J. Physiol.* **277**, R1501-1512.

Veggetti, A., Mascarello, F., Scapolo, P.A. and Rowlerson, A. (1990). Hyperplastic and hypertrophic growth of lateral muscle in *Dicentrarchus labrax* (L.) An ultrastructural and morphometric study. *Anat. Embryol*. **182**, 1-10.

Walesby, N.J. and Johnston, I.A. (1980). Fibre type in the locomotory muscles of an Antarctic teleosts, *Notothenia rossii*. *Cell Tissue Res.* **208**, 143-164.

Weatherly, A.H. and Gill, H.S. (1985). Dynamics of size increase in muscle fibers in teleosts in relation to size and growth. *Experientia* **41**, 353-354.

West, G.B., Brown, J.H. and Enquist, B.J. (1999). The fourth dimension of life: fractal geometry and allometric scaling of organisms. *Science*. **284**, 1677-1679.

Zimmerman, A. and Lowery, M.S. (1999). Hyperplastic development and hypertrophic growth of muscle fibers in the white seabass (*Atractoscion nobilis*). *J. Exp. Zool.* **284**, 299-308.